# Journal Pre-proof


Magnesium-pretreated Periosteum for Promoting Bone-tendon Healing after Anterior Cruciate Ligament Reconstruction

Jiali Wang, Jiankun Xu, Xinluan Wang, Liyuan Sheng, Lizhen Zheng, Bin Song, Ge Wu, Ri Zhang, Hao Yao, Nianye Zheng, Michael Tim Yun Ong, Patrick Shu-hang Yung, Ling Qin

PII: S0142-9612(20)30822-X

DOI: https://doi.org/10.1016/j.biomaterials.2020.120576

Reference: JBMT 120576

To appear in: *Biomaterials*

Received Date: 20 February 2020

Revised Date: 1 September 2020

Accepted Date: 21 November 2020

Please cite this article as: Wang J, Xu J, Wang X, Sheng L, Zheng L, Song B, Wu G, Zhang R, Yao H, Zheng N, Yun Ong MT, Yung PS-h, Qin L, Magnesium-pretreated Periosteum for Promoting Bone-tendon Healing after Anterior Cruciate Ligament Reconstruction, *Biomaterials*, https://doi.org/10.1016/j.biomaterials.2020.120576.

**Wang Jiali, Xu Jiankun, Qin Ling:** Conceptualization, Methodology, Software, Writing-Original draft preparation, Writing- Reviewing and Editing. **Wang Xinluan, Sheng Liyuan, Zheng Lizhen**: Data curation, Writing- Original draft preparation. **Song Bing, Wu Ge, Zhang Ri, Yao Hao, Zheng Nianye, Michael Tim Yun Ong, Patrick Shu-hang Yung**: Visualization, Investigation. **Qin Ling***:* Supervision.

# Magnesium-pretreated Periosteum for Promoting Bone-tendon Healing after Anterior Cruciate Ligament Reconstruction

Jiali Wang [a,b,1,*], Jiankun Xu [b,1], Xinluan Wang [c], Liyuan Sheng [d], Lizhen Zheng [b], Bin Song [e], Ge Wu [f], Ri Zhang [b], Hao Yao [b], Nianye Zheng [b], Michael Tim Yun Ong [b], Patrick Shu-hang Yung [b], Ling Qin [b,**]

[a] Biomedical Engineering School, Sun Yat-sen University, Guangzhou 510006, PR China

[b] Musculoskeletal Research Laboratory of Department of Orthopaedics & Traumatology and Drug Translational Research Laboratory, Li Ka Shing Institute of Health Sciences, The Chinese University of Hong Kong, Hong Kong SAR, PR China.

[c] Translational Medicine R&D Center, Institute of Biomedical and Health Engineering, Shenzhen Institutes of Advanced Technology, Chinese Academy of Sciences, Shenzhen, PR China

[d] Shenzhen Institute, Peking University, Shenzhen, Guangdong province, 518057, PR China

[e] Department of Sports Medicine, Sun Yat-Sen Memorial Hospital, Sun Yat-Sen University, Guangzhou 510006, PR China

[f] Department of Mechanical and Biomedical Engineering, City University of Hong Kong, Kowloon, Hong Kong, PR China.

**ABSTRACT:** Periosteum can improve tendon-bone healing when applied to wrap the tendon graft in both animal studies and clinical trials. As magnesium (Mg) ions can significantly elevate the levels of relevant cytokines involving in the osteogenic differentiation of periosteum-derived stem cells, the Mg-pretreated periosteum may be an innovative approach for enveloping the tendon graft. To test this hypothesis, we compared the effects of Mg-pretreated periosteum (M-P) and the stainless steel (SS)-pretreated periosteum (SS-P) in ACL reconstruction. We firstly found that the released Mg ions from the Mg implants were partially accumulated in periosteum, resulting in higher Mg/Ca ratio in the M-P compared to the SS-P. Additionally, the M-P showed significantly higher expression levels of calcitonin gene-related peptide (CGRP) and periostin than the SS-P due to the decrease in Cathepsin K (CTSK). Elevation of CGRP and periostin was beneficial for the osteogenic differentiation of periosteum-derived stem cells. More importantly, we demonstrated that the M-P remarkably increased the formation of fibrocartilage at the interface between the periosteum and tendon. Collectively, M-P group demonstrated significantly prevented peri-tunnel bone loss, more osseous ingrowth into the tendon graft and higher maximum load to failure as compared to the SS-P group. In summary, our study warrants further investigations for translating the current proof-of-concept findings to optimize the delivery of CGRP, periostin, and cells as novel practical therapeutic strategy for enhancing tendon-bone interface healing in patients undergoing ACL reconstruction.

[1] The authors contributed equally to this work.

* Corresponding author. School of Biomedical Engineering, Sun Yat-sen University, Guangzhou, China.

**Corresponding author. Musculoskeletal Research Laboratory, Department of Orthopaedics & Traumatology, The Chinese University of Hong Kong, Hong Kong SAR, China.

*E-mail addresses*: qin@ort.cuhk.edu.hk (Qin L) or wangjli8@mail.sysu.edu.cn (Wang J).

**Keywords**: ACL reconstruction; CGRP; Magnesium; Periosteum; Macrophages

## 1. Introduction

Patients with anterior cruciate ligament (ACL) injuries are at higher risk of developing osteoarthritis (OA) due to deterioration of knee stability [1, 2]. ACL reconstruction has been established for over 30 years for reducing meniscal injuries and avoiding knee replacement in the long run [3]. However, there is still an average failure rate of 11.9 % for ACL reconstruction [4]. A meta-analysis of 69 studies showed that only 81% patients were able to return to moderate sport after surgery [5]. Apart from technical failures, insufficient tendon graft-bone healing has been considered as one of the main causes for the unsatisfactory clinical outcomes [6]. Rodeo et al. reported a positive correlation between the tendon graft-bone interface strength and the degree of bony ingrowth, mineralization, and tissue maturation at the interface [7]. Currently, a variety of biological factors, including bone morphogenetic proteins (BMPs) [8], transforming growth factors (TGF)-β superfamily [9], platelet-derived growth factor-BB (PDGF-BB) [10], vascular endothelial growth factor (VEGF) [11], granulocyte colony stimulating factor (G-CSF) [12], and platelet rich plasma (PRP) [13], have been applied to enhance the osteointegration of the tendon graft into the bone tunnels in animal models and patients. However, their clinical applications are still limited because of the controversy in the outcomes [14]. More importantly, it is very difficult to maintain these growth factors at a favorable concentration in the target region. The use of autologous tissue, which possess cells and favorable cytokines involving in repair, may exert beneficial effects on the healing.

Periosteum, as a pool of stem cells and osteoblastic precursors, supports both chondrogenesis and osteogenesis during bone repair [15], suggesting its potential in the enhancement of tendon-bone healing. Recently, Chen et al. reported the encouraging outcomes from both preclinical and clinical studies after using periosteum to wrap the tendon graft before inserting into the bone tunnel during ACL reconstruction [16-18]. However, as only 85% patients could return to moderate activity after surgery, it is still far away from the satisfactory clinical outcomes in terms of activity level after reconstruction using the non-pretreated periosteum. Our previous study demonstrated that the release of calcitonin gene-related peptide (CGRP), a neuropeptide with great contributions in the promotion of osteogenic differentiation of precursor cells via activating the cyclic adenosine 3',5'-monophosphate (cAMP)/cyclic adenosine monophosphate response element-binding protein (CREB) pathway, was significantly enhanced in the periosteum with the presence of higher concentration of magnesium (Mg) ions [19, 20]. Besides, higher Mg could significantly enhance the cell adhesion strength via activating integrin/focal adhesion kinase (FAK) signaling pathway [21]. As a predominant extracellular protein in the periosteum, periostin can mediate cell migration and adhesion through the integrin/FAK pathway [22]. Thus, Mg ions may also affect the secretion of periostin in periosteum derived stem cells (PDSCs). Recent

study revealed that periostin could control bone regenerative potential via upregulating the osteogenic differentiation of PDSCs [23]. Taken together, we raised a hypothesis here that the PDSCs from the Mg-pretreated periosteum might possess promoted osteogenic differentiation capability attributing to the elevation of CGRP and periostin in the periosteum, which might ultimately lead to enhanced tendon graft-bone healing.

## 2. Materials and methods

### 2.1 *In vivo* studies in rabbits and rats

The animal experiments were approved by the Animal Experimentation Ethics Committee of the Chinese University of Hong Kong (AEEC No. 17-010-MIS). High-purity Mg (E-ande, Dongguan, China) or commercial stainless steel (SS) (commercial purity, Baoji Xinnuo New Metal Material, Baoji, China) rods with 3 mm in diameter were inserted into the femoral cavities of the skeletally mature male rabbits. The periosteum was harvested at week 1, 2 and 3 after surgery for immunofluorescent staining and quantitative measurement of CGRP. In addition, the periosteum pretreated by Mg or SS rods (referred to M-P group and SS-P group, respectively) for 2 weeks was used to wrap the long digital extensor tendon autograft for ACL reconstruction in the contralateral knee (**Fig. S1**). Forty-four rabbits were then sacrificed by a lethal injection of concentrated sodium pentobarbital after general anesthesia at week 4 and 8 after ACL reconstruction. As our previous studies indicated that the tendon graft failed in the mid-substance over 6 weeks after surgery in the tensile testing [24], 6 of the 14 rabbits at week 4 from both the SS-P and M-P groups were used for biomechanical testing to compare their tensile properties of tendon graft-bone complex. The remaining 8 rabbits in each group were used for radiographic assessment prior to histological evaluations on both decalcified and undecalcified sections. At week 8 after reconstruction, 8 rabbits in each group were used for radiographic and histological assessments. Besides, in another set of study, to explore the contributions of the SS-P and M-P to the tendon graft-bone healing, the SS-P and M-P collected from the femur was used to wrap around the long digital extensor tendon in the contralateral knee and then tightly sutured. The periosteum-tendon complex was harvested at week 2, 3 and 4 after surgery for histological analysis. Similarly, Mg or SS pins with 1.2 mm in diameter were inserted into the femoral cavities in skeletally mature female rats for immunohistochemical staining, immunofluorescent staining, element analysis, and gene/protein detection.

#### *2.1.1.ACL reconstruction surgery in rabbits*

As shown in **Figure 1A(a-d)**, the pretreated periosteum (about 10 mm×10 mm) was stripped from the outer layer of the right femur of rabbits and then kept in the sterilized phosphate buffer saline (PBS). A 2-3 cm skin incision next to the patellar tendon on the lateral side was created to harvest the long digital extensor tendon graft. Then, a medial parapatellar arthrotomy was performed to expose the knee joint prior to patellar dislocation. The infrapatellar fat tissue was removed to expose the joint cavity for ACL transection. After that, 2.5 mm bone tunnels were created in the femur

and tibia through the footprint of the original ACL by using a bone drill via the transtibial technique for the placement of the harvested tendon graft. The SS-P or M-P was then used to wrap the tendon graft for insertion into the tibial tunnel prior to the fixation of the two ends of the tendon graft by using non-absorbable sutures. In order to label the newly formed bone, 4 rabbits from each group were administered with xylenol orange (90 mg/kg) at 21 days and 49 days after surgery via muscular injection for 4-week and 8-week time points, respectively [25].

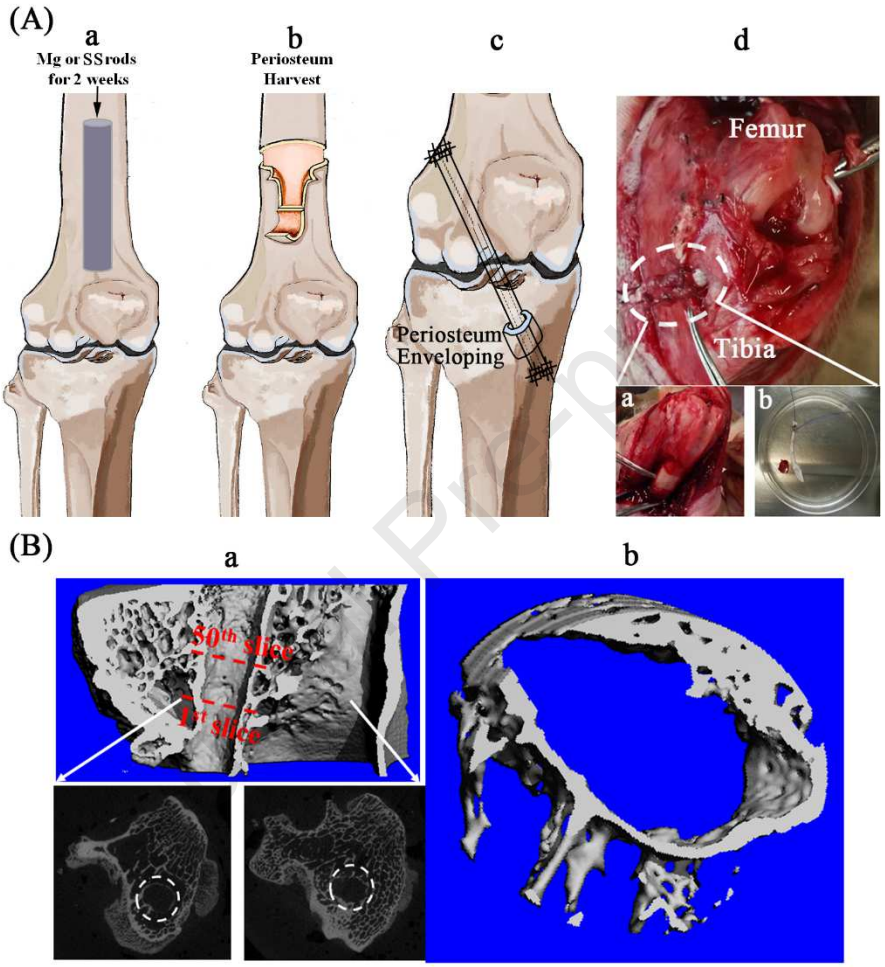


**Figure 1**. Surgical design and CT scanning protocol. (A) The SS-P or M-P (a-b) of the femora in rabbits were harvested to wrap the tendon graft for ACL reconstruction in the contralateral knee (c-d). (B) Radiographic analysis of the peri-tunnel bone tissue in the tibia. (a) A total number of 50 slices (indicated by the red dotted line) were segmented for creating 3D images of the ROIs outlined in the starting slice and the last slice by the white dotted circle. (b) 3D reconstruction of the peri-tunnel bone tissue.

*2.1.1.1.Immunofluorescent staining and quantitative measurement of CGRP by ELISA*

The periosteum harvested at week 1, 2 and 3 after implantation in both the M-P and SS-P groups were divided into two parts. One part was immersed into 95% ethanol for fixation prior to dehydration in 30% sucrose solution. Cryosections with 5 μm in thickness were prepared for immunofluorescence staining of CGRP (Abcam, USA). Another part was lysed in RIPA lysis buffer (Thermo Fisher Scientific, USA)

supplemented with protease and phosphatase inhibitors (Thermo Fisher Scientific, USA). The supernatant was collected for BCA protein quantitative analysis and then used for the quantitative detection of CGRP by ELISA kit (Abebio, China). The CGRP concentration was normalized by the levels of the total protein.

*2.1.1.2.Micro-CT analysis*

The harvested tibiae were fixed in the sampling tube of a high-resolution micro-computed tomography system (Viva CT 40, Scanco Medical, Brüttisellen, Switzerland) before scanning. The parameters for X ray-tube were set as following: 55 kV (tube voltage), 145 μA (tube current), 30 μm (an isotropic voxel size) [24]. A region of interest (ROI) with 4 mm in diameter was selected at the center of the bone tunnel for 3D image construction (**Figure 1B(a-b)**). A series of 2D tomographic gray-images (50 slices) along the direction perpendicular to the bone tunnel were segmented for 3D reconstruction of the peri-tunnel bone tissue. Prior to 3D reconstruction of selected volume of interest in bone tissue, the resulting gray-images were segmented using a fixed threshold and a low-pass filter to minimize the noise (Sigma = 1.2, support = 2.0, threshold = 160). In the reconstructed peri-tunnel bone tissue, relative bone volume (BV/TV), trabecular number (Tb. N), trabecular thickness (Tb. Th), trabecular separation (Tb. Sp), connectivity density (Conn. D), and specific bone surface (BS/BV) were reported [24].

*2.1.1.3.Histological and histomorphometric analysis*

Forty-four rabbit tibiae were fixed in 4% neutral buffer formalin for 48 hrs and then divided into decalcified and undecalcified groups. The samples were processed according to our previously published protocol [21]. For the decalcified group, the samples were decalcified with 15% EDTA (pH 7.4) at room temperature for 3 months, and then embedded with paraffin. A 5 μm-thick paraffin section was obtained from the central portion of the bone tunnel and stained with hematoxylin & eosin (H&E). The tibiae assigned to the undecalcified group were directly embedded into methylmethacrylate (MMA) after dehydration in a series of graded ethanol and xylene. Stevenel blue-Van Gieson-Alizarin Red S (SVA) staining and Golder's trichrome staining were performed in thick (approximate 100 μm) and thin (10 μm) MMA sections, respectively [21]. The images were captured under the microscopy (DM 5500B, Leica, Germany). The newly formed bone at the tendon-bone interface and the interface width were measured using Image J (1.47 t, NIH, USA). In addition, a 5 μm-thick MMA section was observed by fluorescence microscopy (DM 5500B, Leica, Germany). The area ratio of new bone in the peri-tunnel tissue was calculated via measuring the fluorescent positive area in the fluorescence images and the total bone area in the white light images, respectively.

In order to detect the histological responses at the interface between the periosteum and the tendon in the periosteum-tendon complex, a 5 μm-thick paraffin section was prepared for H&E and Safranin O & Fast green (S&F) staining.

*2.1.1.4.Tensile testing*

The femur-tendon graft-tibia complexes (FTGTC) were harvested and then stored at -80 °C. Before biomechanical testing, the samples were thawed in 4 °C cold room overnight. Excluding the ACL graft, excess soft tissues in FTGTC were carefully removed. Afterwards, the specimens were mounted on the custom-designed jigs in a uniaxial mechanical testing machine (H25K-S, Hounsfield Test Equipment LTD, Surrey, UK). The tensile tests were then conducted on the samples with the knee flexed to 90° according to previously published protocols with a preload of 1 N and a rate of 50 mm/min until failure [24]. The maximal load to failure and the failure mode were recorded for all the samples, with a sample size of n=6 for each group.

### *2.1.2. In vivo* studies in rats

Mg or SS pins (1mm in diameter) were inserted into the femoral cavities of 3-month-old male rats for the following assessments.

*2.1.2.1.μX-ray fluorescence (μXRF) measurements*

μXRF measurements were conducted using scanning X-ray microscope (Grenoble, France). The step width was set as 5 μm for generating the XRF maps (25 adjacent lines with 5 μm spacing). The use of the dual-energy X-ray beam configuration allowed for high excitation of Mg and Ca with the 2.1 keV and 6.3 keV energy part of the X-ray beam, respectively. To analyze the spatial changes in Mg concentrations along the bone tissue, the Mg/Ca ratio was calculated based on the line scans performed from the bone-marrow cavity to the periosteum.

*2.1.2.2.Extraction of RNA from periosteum for qRT-PCR*

At week 2 post implantation, three rats from each group were sacrificed using overdose of phenobarbital. The periosteal tissues at the regions with Mg or SS implantation were freshly harvested and cut into two equal parts. One part was homogenized in RNAiso Plus (TaKaRa) for further RNA extraction. The expression levels of osteoclastic gene (*Ctsk*) and osteogenic genes (*Spp1*, *Bglap*) were measured using qRT-PCR. The sequences of used primers were listed in Table 1.

Table 1. Primer sequences

| Gene | Forward primer (5’-3’) | Reverse primer (5’-3’) |
|---|---|---|
| *Ctsk* | TTCCTCAACAGTGCAAGCGA | TCCAGCGTCTATCAGCACAG |
| *Spp1* | AGGCGCATTACAGCAAACAC | CTCGCTCTCTGCATGGTCTC |
| *Bglap* | CTAGCGGACCACATTGGCTT | CAGCTGTGCCGTCCATACTT |
| *Gapdh* | GGCTCATGACCACAGTCCAT | ACATTGGGGGTAGGAACACG |

*2.1.2.3.Extraction of protein from periosteum for western blotting*

Another part of periosteal tissues mentioned above were homogenized in RIPA buffer for extracting total protein. The periostin expressions between M-P and SS-P groups were quantified using western blotting. In addition, we also measured the periostin expression in tissue lysis after incubating with recombinant human cathepsin K protein (active form, ab157067, Abcam, USA) for 4 hrs. We further measured the

remaining of recombinant human periostin protein (ab203522, Abcam, USA) with set initial concentration (0.5 μg/μl) after mixed with active form of cathepsin K protein (0.5 μg/μl) for two time points at 4 hrs and 8 hrs. Anti-Periostin antibody (ab14041, Abcam, reacts with both rat and human, USA) was used at a dilution of 1: 100.

*2.1.2.4.Specific staining of periostin and CD206 at the periosteal layer*

The harvested rat femora in both M-P and SS-P groups were fixed and decalcified for preparing paraffin sections cut at 5 μm in thickness for either immunohistochemical or immunofluorescent staining of periostin and CD206 (both from Abcam, USA), respectively.

## 2.2. *In vitro* studies

*2.2.1. Isolation of PDSCs and osteogenic differentiation assay*

To investigate if PDSCs were involved in the enhanced healing during the tendon-bone integration, we isolated primary PDSCs from the SS- or Mg-pretreated femoral periosteum of the rats at 2 weeks after surgery according to a published protocol [23]. Briefly, the epiphyses were cut off for complete removal of the bone marrow by repeatedly washing with PBS. Then, the bone graft was cultured in the cell culture medium for the migration of PDSCs. After 2 weeks, the bones were removed and PDSCs were trypsinized for the *in vitro* studies. For osteogenic differentiation, the cells were seeded in a 6-well plate at a density of $5\times10^4$ cells/well and cultured in basal complete culture medium until the cells reached 90% confluence. Cells were then incubated in osteogenic medium, which contained basal complete medium, 10 mM β-glycerophosphate, 50 μM ascorbic acid and 10 nM dexamethasone (all from Thermo Fisher Scientific, USA). ALP staining (BCIP/NBT, Sigma) and quantitative real-time polymerase chain reaction (qRT-PCR) for the measurement of *Bglap* and *Sppl* mRNA were performed on day 7.

PDSCs from SS-P group were used to investigate if supplementation of recombinant periostin (ab203522, Abcam) could affect their osteogenic differentiation. The dosages of periostin were set at 0 ng/ml (as control), 50 ng/ml and 100 ng/ml in osteogenic medium, according to a previous study [26]. The medium was changed every other day. On day 21, the cells were processed to protein extraction by following the protocol as mentioned in section 2.1.2.3. Then the expression levels of osteogenic markers (Runx2, Osterix, and Osteocalcin) were analyzed by western blot, according to our established protocols [19, 27, 28].

*2.2.2. Culture of RAW 264.7 cells and isolation of bone marrow derived macrophages (BMM) for osteoclastic differentiation*

RAW264.7 cells (5000 cells/$cm^2$) were cultured in DMEM/F12 (D8900-10L, Life Science, Sigma-Aldrich, USA) containing 10% FBS, 1% PSN antibiotic mixture (Gibco™, Thermo Fisher Scientific, USA) and receptor activator of nuclear factor kappa-B ligand (RANKL) (20 ng/mL) for 4 days to induce osteoclastic differentiation. In addition, the bone marrow from bilateral femora of rats was washed out and cultured at 37 □ containing 5% $CO_2$ for 2 hrs. Un-adherent cells were then transferred

and cultured in the cell culture medium supplemented with 20 ng/ml macrophage colony-stimulating factor (M-CSF) (SRP3247, Sigma-Aldrich, USA) for 48 hours. Then Cells was passaged to 12-well-plate (300,000/well) with 20 ng/ml M-CSF and 20 ng/ml RANKL (PHP0034, Thermo Fisher Scientific, USA) for 48 hours for osteoclastic differentiation. For both BMMs and RAW 264.7 cells, cell culture medium with different Mg ion levels (0.8 mM and 10 mM) was used. Then qRT-PCR analysis and tartrate-resistant acid phosphatase (TRAP) staining (387A-1KT, Sigma-Aldrich, USA) were conducted in both BMMs and RAW 264.7 cells after osteoclastic differentiation.

*2.2.3. Macrophages polarization assays*

RAW264.7 cells (5000 cells/cm$^2$) were cultured in 10-cm dish containing DMEM/F12 (D8900-10L, Life Science, Sigma-Aldrich, USA) supplemented with 10% FBS, 1% PSN antibiotic Mixture (Gibco™, Thermo Fisher Scientific, USA). After 48 hrs, 20 ng/ml IL-4 with and without 10 mM Mg ions [29] was used to generate M2-type macrophages. After 12 hrs, the cells were washed twice with PBS prior to cell suspension. Then the cells were incubated with the anti-CD206 antibody and the FITC conjugated secondary antibody (both from Abcam, USA) for flow cytometry analysis. Cells which were not incubated with any antibody were used as blank controls.

To validate the finding from macrophage cell line, primary bone marrow macrophages isolated in section 2.2.2 were used. For M1 stimulation, the culture medium was supplemented with 100 ng/ml LPS; for M2 stimulation, supplemented with 20 ng/ml IL-4. For the experimental group, 10 mM Mg ions were supplemented. After stimulating for 24 hrs, the expressions of iNOS and CD206 were measured by immunofluorescent staining with corresponding antibodies (anti-iNOS antibody, ab3523, abcam; anti-CD206 antibody, ab64693, abcam).

### 2.3. Statistical Analysis

All data were expressed as mean ± standard deviation (SD), with the significant level set as $P < 0.05$. The unpaired two-tailed Student's *t*-test was used for comparing the data between two groups. One-way analysis of variance (ANOVA) with Bonferroni *post-hoc* tests were conducted for comparing the data from multiple groups.

## 3. Results

In the whole project, there was no complication in rabbits in both the M-P and SS-P groups after surgery. No cartilage degeneration was observed in the operated knee joint.

### 3.1. The accumulation of Mg ions in the periosteum upregulated CGRP and Periostin expression

According to the line scans of Mg and Ca elements using μXRF, a higher Mg/Ca ratio was detected in the cortical bone of the Mg-inserted femora when compared to those without Mg insertion and or SS-insertion. More importantly, a dramatic increase of

Mg/Ca ratio was recorded at the interface between periosteum and bone in the Mg-inserted group, indicating the diffusion and subsequent storage of the released Mg ions within the periosteum **(Figure 2A**). As compared to the SS-P, the M-P showed enhanced expression of CGRP according to immunofluorescent staining (**Figure 2B**). In addition, the CGRP labelling intensity in the M-P group increased within the first 2 weeks while decreased at week 3, indicating a time-dependent release of CGRP under the stimulation of Mg ions. ELISA results were consistent with the immunofluorescence staining findings. The CGRP level was kept stable in the periosteum of the SS-P group while it reached the peak at week 2 in the M-P group, with about 2-fold higher CGRP level than the SS-P group (**Figure 2B**). At week 3, the expression of CGRP in the M-P group was lower than that of week 2, suggesting that week 2 is the optimal time point for harvesting periosteum for ACL reconstruction. The periostin expression level calculated as the periostin positive area ratio in periosteum of rats, was significantly higher in the M-P group than that of the SS-P group at week 2 after implantation (**Figure 2C**). However, there was no significant difference found in periostin positive area ratio between the two groups at week 3 after surgery.

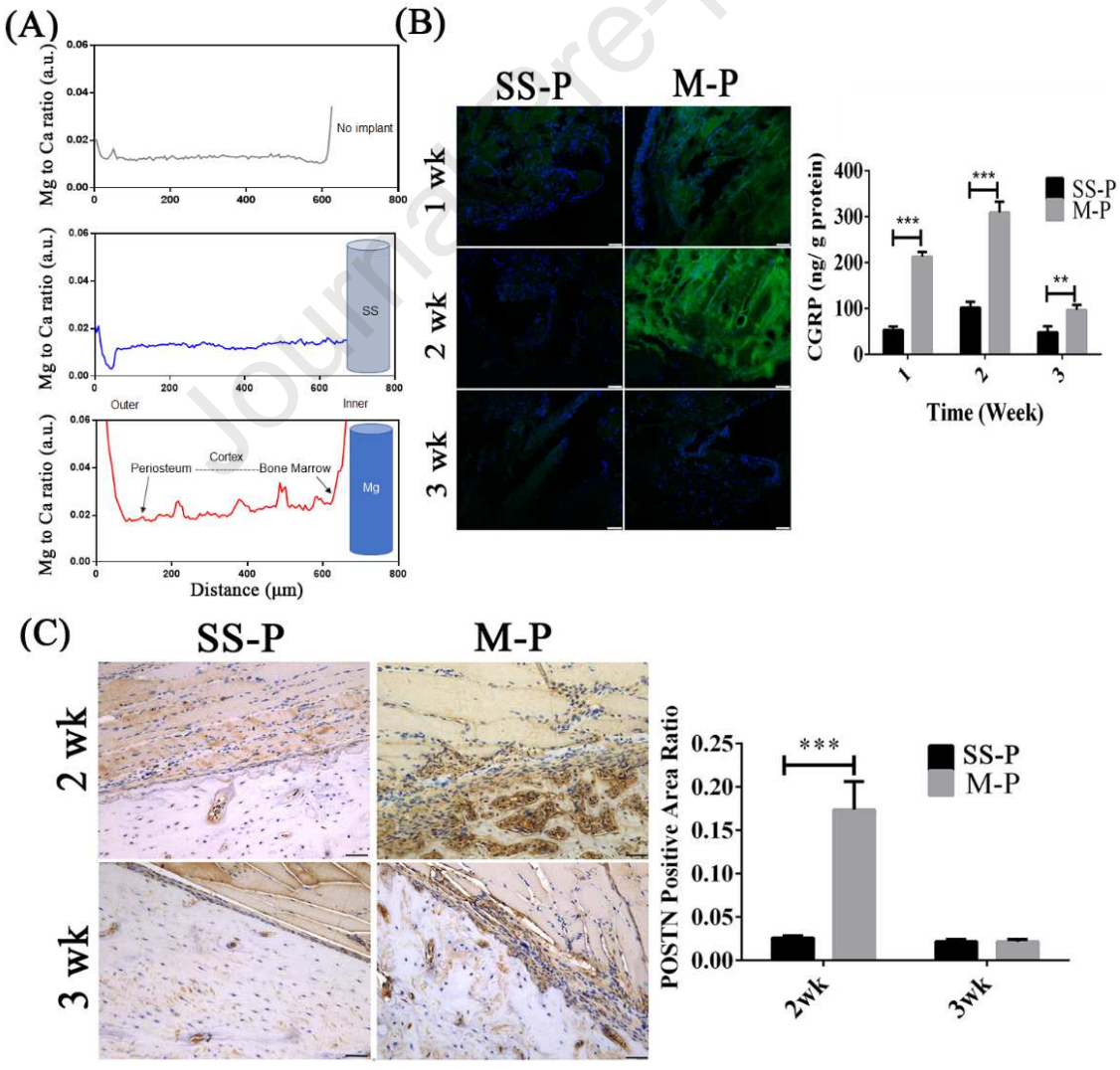

**Figure 2** Effects of Mg ions on the expressions of CGRP and Periostin in the periosteum. (A) μXRF line scanning for recording the ratios of Mg to Ca from bone marrow to periosteum in the femora with or without pretreatment of SS or Mg pins for 2 weeks. (B) Representative immunofluorescent labeling and ELISA analysis for CGRP in the periosteum of rabbits pretreated with SS or Mg rods in femora for 1, 2, and 3 weeks, respectively. n=3, ***P*<0.01, ****P*<0.001. Scale bars, 50 μm. (C) Immunohistochemical staining and quantitative analysis of periostin in the periosteum of the SS-P and M-P groups at week 2 and 3 after implantation. n=3. ****P*<0.001. Scale bar, 100 μm

### 3.2. Mg-pretreated periosteum (M-P) promoted the osteointegration of the tendon graft into the bone tunnel and prevented peri-tunnel bone loss

Fibrocartilage zone was observed at the tendon-bone interface in the M-P group while only fibrous tissue was formed at the interface in the SS-P group at week 4 after surgery (**Figure 3A(a-b)**). At week 8 after surgery, more osseous ingrowth into the interface was found in the M-P group (**Figure 3A(a-b)**), exhibiting significantly greater area of newly formed bone at the tendon-bone interface when compared to the SS-P group (**Figure 3A(c)**). The fibrous interface width at the tendon-bone interzone structure, which has been recognized as a negative factor affecting the tendon-bone healing quality [30], was also evaluated in this study. As shown in **Figure 3A(d)**, the fibrous interface was observed in both the SS-P and M-P groups at week 4 after surgery, which was then followed by a reduction in the width of the fibrous interface in both groups at week 8 after operation. Compared to the SS-P group, the M-P group showed significantly narrower fibrous interface width at week 4 after surgery (**Figure 3(e)**). However, no significant difference was observed in the fibrous interface width between the two groups at week 8 after surgery.

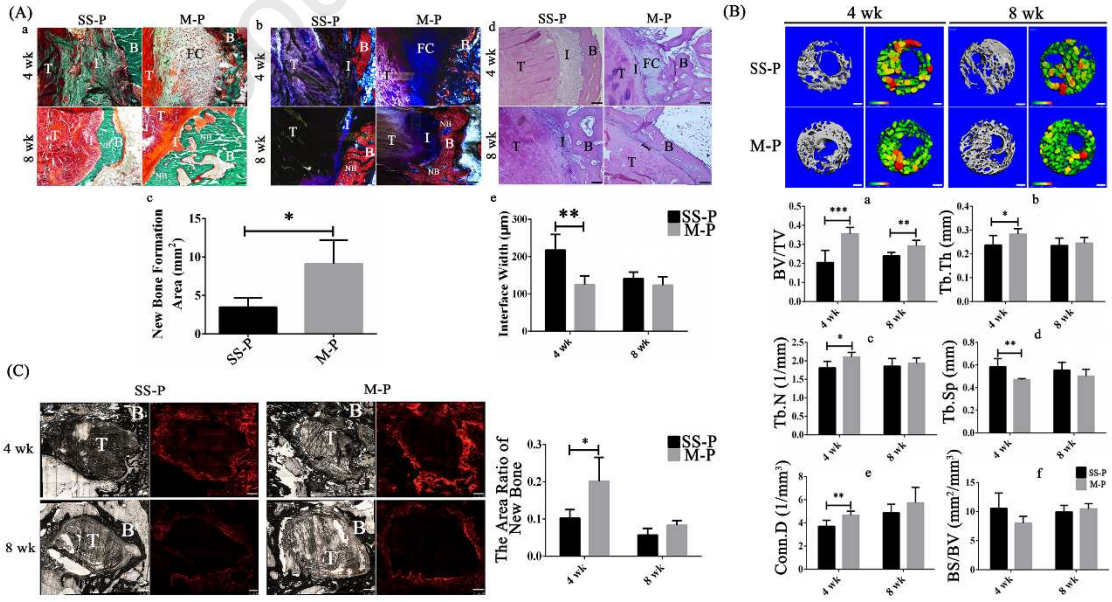


**Figure 3**. Effects of periosteum on tendon-bone healing and the peri-tunnel bone loss. (A) Histological analysis of the tendon-bone interface at the tibial tunnel in both the SS-P and M-P groups at week 4 and 8 after surgery. a. Goldner's Trichrome staining of tendon-bone interzone

structure. b. Stevenel blue-Van Gieson-Alizarin Red S staining of tendon-bone interface. c. The new bone formation area at the tendon-bone interface in both the SS-P and M-P groups at week 8 after surgery. n=4. *$P$<0.05. d. H&E staining of tendon-bone interface. e. The width of the fibrous tissue formed at the tendon-bone interface in both the SS-P and M-P groups at week 4 and 8 after surgery. n=4. **$P$<0.01. T: tendon graft; I: interface; B: bone; FC: fibrocartilage; NB: new bone. Scale bar: 100 μm. (B) The 3D reconstruction and structural parameters of the peri-tunnel bone tissue in the tibiae as measured by micro-CT at week 4 (4 wk) and week 8 (8 wk) after surgery. a: Bone volume fraction (BV/TV); b: Trabecular thickness (Tb. Th); c: Trabecular number (Tb. N); d: Trabecular separation (Tb. Sp); e: Connectivity density (Conn. D); f: Specific bone surface (BS/BV). n=6. *$P$<0.05, **$P$<0.01, ***$P$<0.001. (C) Representative images showing the new bone formation in the peri-tunnel region via fluorescent labelling and quantitative analysis of the newly formed bone area in both the SS-P and M-P groups at week 4 and week 8 after surgery. T: tendon graft; B: bone. White scale bar: 500 μm. The area ratio of new bone was defined as the ratio of the fluorescent signal positive area and the bone area in the fluorescence and bright field images. n=4. *$P$<0.05.

As shown in **Figure 3B**, the 3D reconstructions of the peri-tunnel tissue showed that the M-P group exerted significantly higher BV/TV than the SS-P group at week 4 (0.36±0.03 vs. 0.21±0.06, $P$<0.001) and week 8 (0.29±0.03 vs. 0.24±0.02, $P$<0.01) after surgery. In addition, there were significant differences in the trabecular thickness (Tb. Th), trabecular number (Tb. N), trabecular separation (Tb. Sp) and connectivity density (Conn. D) between the SS-P group and the M-P group (Tb. Th: 0.28±0.02 mm vs. 0.23±0.04, $P$<0.05; Tb. N: 2.10±0.13 vs. 1.80±0.17, $P$<0.05; Th. Sp: 0.47±0.01 mm vs. 0.59±0.07 mm, $P$<0.01; Conn. D: 3.69±0.52 $mm^{-3}$ vs. 4.65±0.35 $mm^{-3}$, $P$<0.01) at week 4 after operation. However, no significant difference was detected in these parameters between the two groups at week 8 after operation. There was no significant difference in the specific bone surface (BS/BV) between the two groups at week 4 and 8 post-surgery.

Besides, the fluorescent labeling examination for the immature bone in the peri-tunnel tissue showed the area ratio of new bone in the peri-tunnel was significantly higher (0.10±0.02 vs. 0.20±0.06, $P$<0.05) in the M-P group when compared to the SS-P group at week 4 after surgery (**Figure 3C**). Even at week 8 after operation, the area ratio of new bone was still higher in the M-P though yet with marginal statistical difference (0.06±0.02 vs. 0.08±0.01, $P$=0.051).

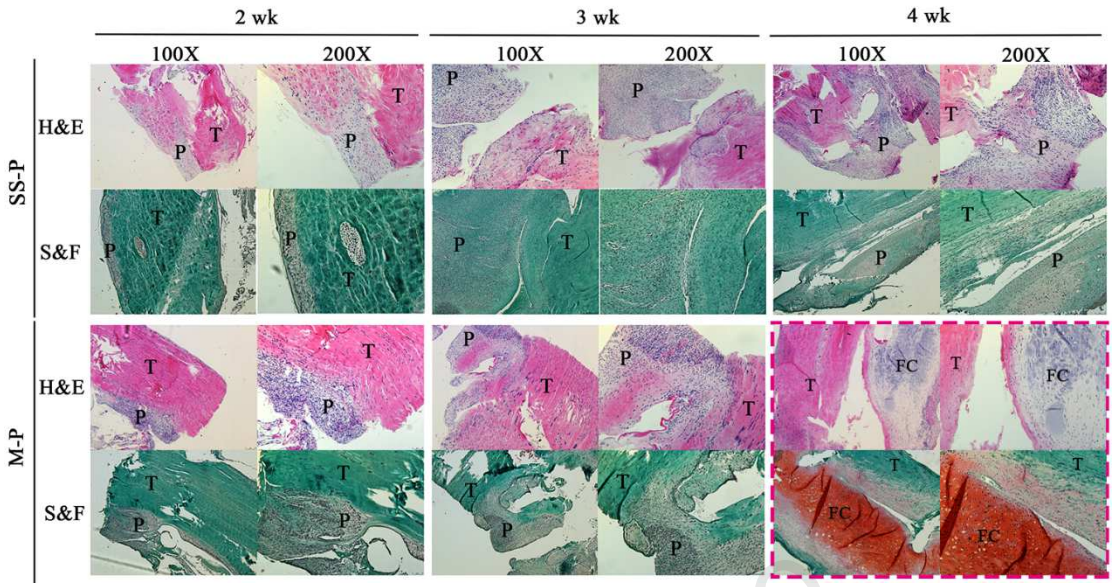


**Figure 4**. Representative histological sections from SS- or Mg-pretreated periosteum-tendon graft complex harvested at week 2, 3 and 4 after surgery (H&E and S&F staining; Magnification: 100× & 200×. Massive fibrocartilage (FC) was present at the complex interface in the M-P group at week 4, which was highlighted by the pink dotted rectangular frame. T: tendon graft; P: periosteum; FC: fibrocartilage. n=2.

In addition, we also wrapped the long digital extensor tendon with periosteum but did not insert the periosteum-tendon construct into bone tunnel, to investigate the interaction of periosteum and tendon, without the interference from bone marrow. H&E and S&F staining results demonstrated that only fibrous tissue was formed at the interface between periosteum and tendon in the SS-P group at all the tested time points (week 2, 3, and 4). There was no difference between SS-P and M-P at week 2 and week 3 after surgery, but a massive fibrocartilage zone was only observed in the M-P group at week 4 (**Figure 4**).

### 3.3. Mg-pretreated periosteum enhanced the mechanical properties of the tendon-bone interface

As the FTGTC failed in the mid-substance over 6 weeks after surgery during the tensile testing [24], the osteointegration quality of the tendon graft into the bone tunnels should be evaluated within an earlier stage after ACL reconstruction. Therefore, the samples harvested at week 4 after operation were used for tensile testing in this study (**Figure 5A**). Regarding to failure modes, all specimens in the SS-P group failed at the tibial tunnel while the samples in the M-P group failed at the femoral tunnel (**Figure 5B**). As the SS- or Mg-pretreated periosteum was used to wrap the tendon graft only at the tibial site, these results suggested improved healing quality at the tendon graft-bone interface in the M-P group that was supported by the significantly higher maximal load to failure in the M-P group as compared with the SS-P group (78.9±5.5 N vs. 56.8±7.0 N, $P<0.05$) (**Figure 5C**).

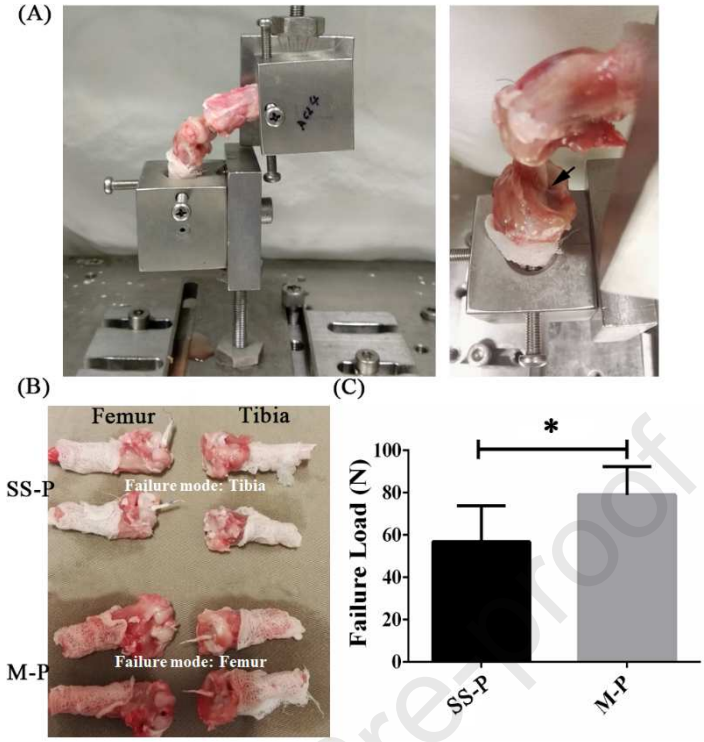


**Figure 5**. Biomechanical testing results. (A) Tensile testing performed in custom-designed jigs for data collection of the maximal load to failure and failure mode in FTGTC. The arrow indicated the failure site. (B) The failure mode in the SS-P and M-P groups at week 4 after surgery. A failure of the tibial fixation in the SS-P group while the failure mode at the femoral side in the M-P was observed. (C) The ultimate failure load in both the SS-P and M-P groups. n=6, **P*<0.05.

### 3.4. Reduced Ctsk expression by Mg degradation led to upregulation of periostin

When analyzing the RNA extracted from periosteal tissues harvested at week 2 post-implantation, qRT-PCR data showed that *Ctsk* mRNA was significantly reduced in M-P than SS-P (**Figure 6A**). *Spp1* (encoding OPN) and *Bglap* (encoding osteocalcin, OCN) exhibited opposite trend (**Figure 6A**). Addition of rhPeriostin elevated the expressions of Runx2, osterix, and OCN during the osteogenic differentiation of PDSCs in a dose-dependent manner (**Figure 6B**), suggesting the direct effect of periostin on osteogenesis. In the protein lysis, the expression of periostin was significantly increased in M-P than SS-P, as measured by western blotting (**Figure 6C**), in agreement with the IHC result (**Figure 2C**). Interestingly, the addition of recombinant human CTSK (rhCTSK) for 4 hrs dramatically decreased the periostin expression in M-P group (**Figure 6C**). Furthermore, when the rhPeriostin was mixed with rhCTSK *in vitro*, it degraded in a time dependent manner (**Figure 6D**). When rhCTSK was added to PDSCs culture for 24 hrs, the expression of endogenous periostin was significantly reduced (**Figure 6E**). These results suggested that the reduced Ctsk expression by Mg might lead to upregulation of periostin.

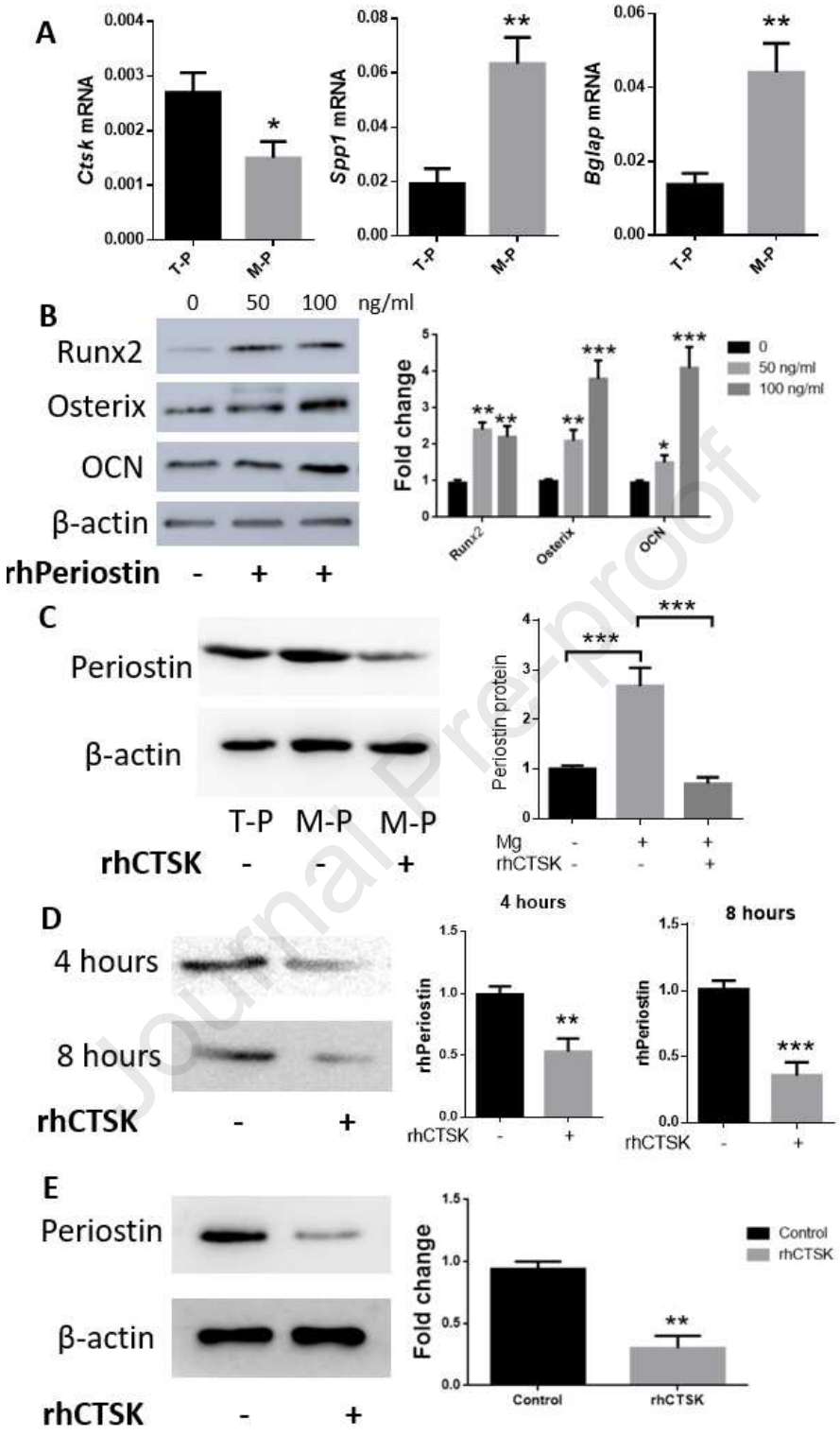


**Figure 6.** The relationship between Ctsk and periostin. (A) mRNA expression of *Ctsk*, *Spp1*, and *Bglap* in rat periosteal tissues isolated at week 2 post-implantation. n=3, **P*<0.05, ***P*<0.01. (B) expression of Runx2, osterix, and OCN on day 21 post-osteogenic induction of PDSCs with rhPeriostin at different doses. The right bar chart was the colorimetric data. n=3, **P*<0.05, ***P*<0.01, ****P*<0.001. (C) Representative western blot of periostin protein expression and the colorimetric data. n=3. ****P*<0.001. (D) Representative western blot of the remaining periostin

protein expression in the solutions mixed with rhCTSK at different time points and the colorimetric data. n=3. ***P*<0.01, ****P*<0.001. (E) Representative western blot showing the expression of endogenous periostin affected by rhCTSK and the colorimetric data. n=3. ***P*<0.01.

### 3.5. Mg treatment enhanced osteogenic differentiation of PDSCs from the periosteum and reduced osteoclast fusion and Ctsk expression levels

As shown in **Figure 7A**, after 7 days of osteogenic differentiation for the isolated PDSCs, the M-P group showed higher expression in ALP than the SS-P group. Besides, the mRNA expression levels of *Bglap* and *Sppl* in the PDSCs of the M-P group were significantly higher than those in the SS-P group (**Figure 7B**). These data suggested that PDSC was at least one of the cell sources mediating the effect of Mg ions. Importantly, the addition of Mg ions into the normal cell culture medium dramatically inhibited the number of osteoclasts from both BMMs and RAW 264.7 cells (**Figure 7C**). Meanwhile, Mg treatment significantly reduced *Ctsk* mRNA expression (**Figure 7C**).

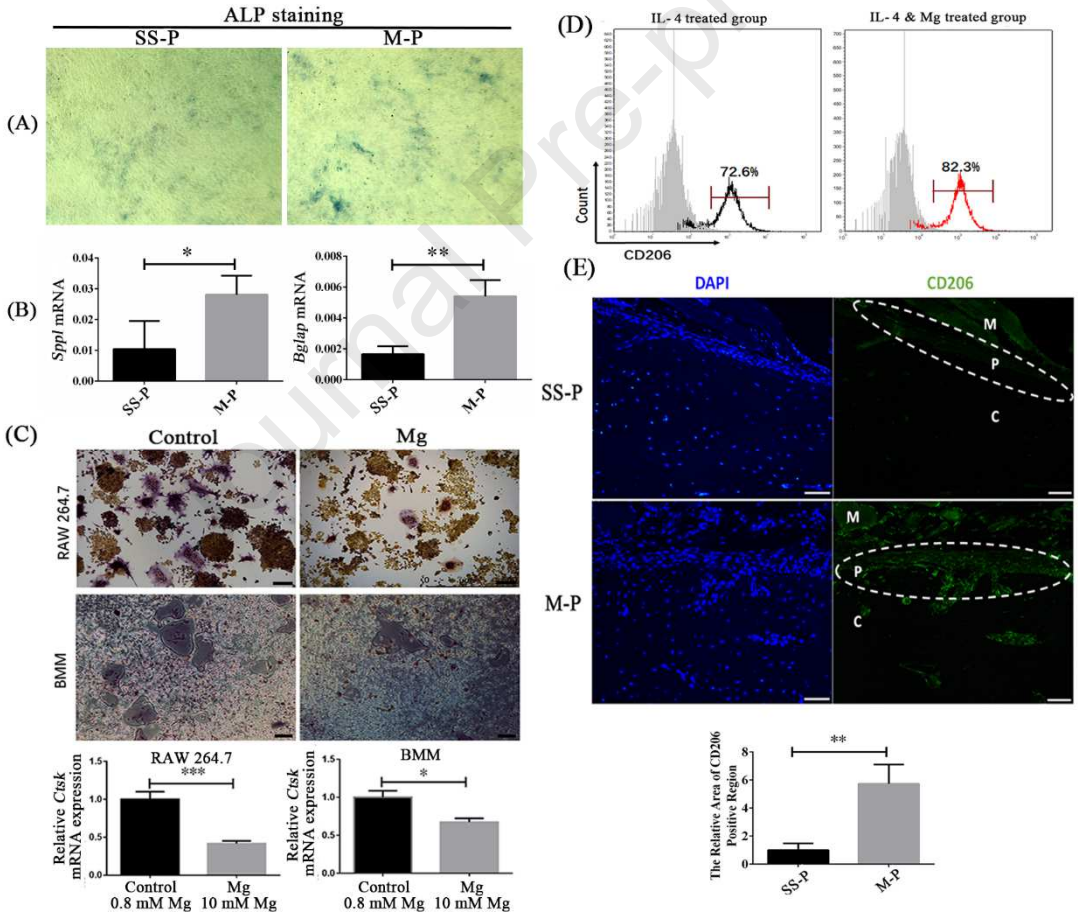


**Figure 7.** Comparisons on the osteogenic differentiation of the primary PDSCs from SS-P or M-P group, osteoclastic differentiation of RAW 264,7 cells and BMM, and macrophage polarization *in vitro* and *in vivo*. (A) Representative images showing ALP staining of PDSCs after 7 days of osteogenic differentiation. (B) RT-qPCR testing results showing significantly higher mRNA expression levels in *Sppl* and *Bglap* in the Mg-induced PDSCs (M-P) when compared to the SS-induced PDSCs (SS-P) after 7-days of osteogenic differentiation. n=4. **P*<0.05, ***P*<0.01. (C)

Effects of Mg ions on osteoclast formation and Ctsk expression levels. n=3. *$P$<0.05, ***$P$<0.001. Black scale bar: 100 μm. (D) Effects of Mg treatment on macrophage polarization in RAW 264.7 cells by flow cytometry analysis. (E) Representative immunofluorescent detection of CD206 positive M2 macrophage at the periosteal layer of the femora in rats with pretreatment of SS or Mg pins for 2 weeks. More M2 macrophages were observed at the periosteum from the M-P group. M: Muscle; P: Periosteum; C: Cortical bone. n=3. **$P$<0.01. Scale bar: 250 μ m.

### 3.6. Mg treatment modulated macrophage towards M2 phenotype

As evidenced by the induction of the M2 macrophage marker, CD206, flow cytometry analysis revealed that Mg ions enhanced M2 macrophage polarization (**Figure 7D**). Similarly, the immunofluorescence analysis of CD206 positive macrophage in the periosteum of rats with SS or Mg pretreatment for 2 weeks also showed that Mg significantly favored macrophages towards M2 phenotype (**Figure 7E**). Consistently, in the primary BMMs, supplementation of Mg ions (10 mM) significantly inhibited M1 polarization (decreased iNOS), while promoted M2 polarization (more CD206 positive cells), as compared to the control with Mg at the physiological concentration (0.8 mM) group (**Figure 8A and 8B**).

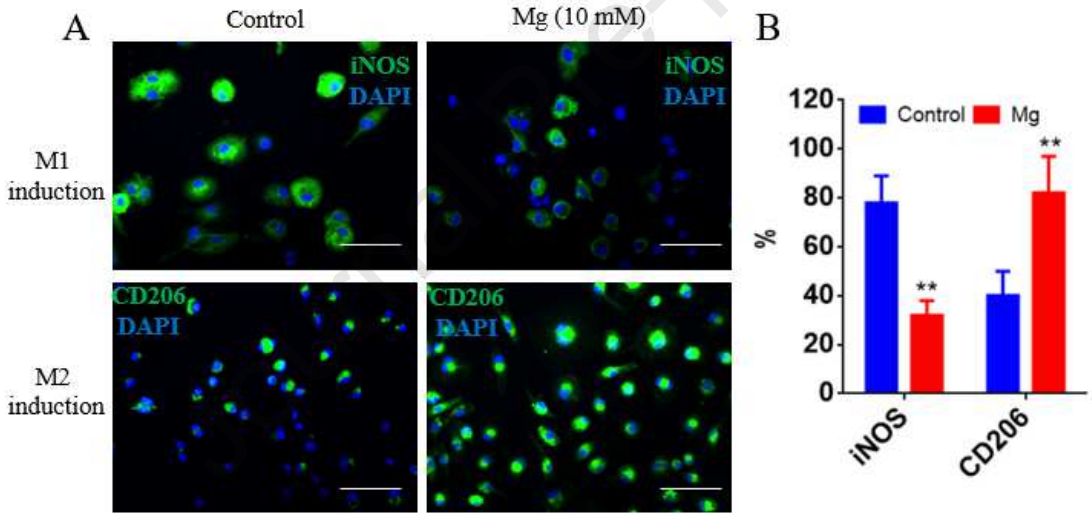


Figure 8. Effects of Mg ions on primary BMMs polarization. (A) Immunofluorescent staining of iNOS and CD206. Scale bar: 100 μm. (B) Significant inhibition of M1 polarization while promotion of M2 polarization by higher Mg ions supported by statistical analysis on the percentage of cells positive for the indicated markers. n=5. **$P$<0.01 as compared to the control.

## 4. Discussion

To the best of our knowledge, this is the first study investigating the effects of Mg-pretreated periosteum on the osteointegration of the tendon graft into the bone tunnels via radiographical, histological, and mechanical measurements in a rabbit ACL reconstruction model. In this study, we found that the PDSCs from the Mg-pretreated periosteum enhanced the tendon graft-bone healing owing to the elevated expressions of CGRP and periostin in the periosteum. As shown in **Figure 9**,

there were three major findings in our current work: Firstly, Mg ions significantly reduced CTSK expression levels, which is beneficial for the upregulation of periostin. Secondly, as compared to the SS-induced periosteum, the Mg-pretreated periosteum showed significantly higher expression levels of CGRP and periostin, which might lead to an improved osteogenic differentiation potential of PDSCs. Thirdly, more new bone formation in the peri-tunnel tissue and enhanced osteointegration of the tendon graft into the bone tunnels were found in the M-P group when compared to the SS-P group. Thus, the Mg-pretreated periosteum is superior to the control periosteum for ACL reconstruction, which in turn is expected to improve clinical outcomes.

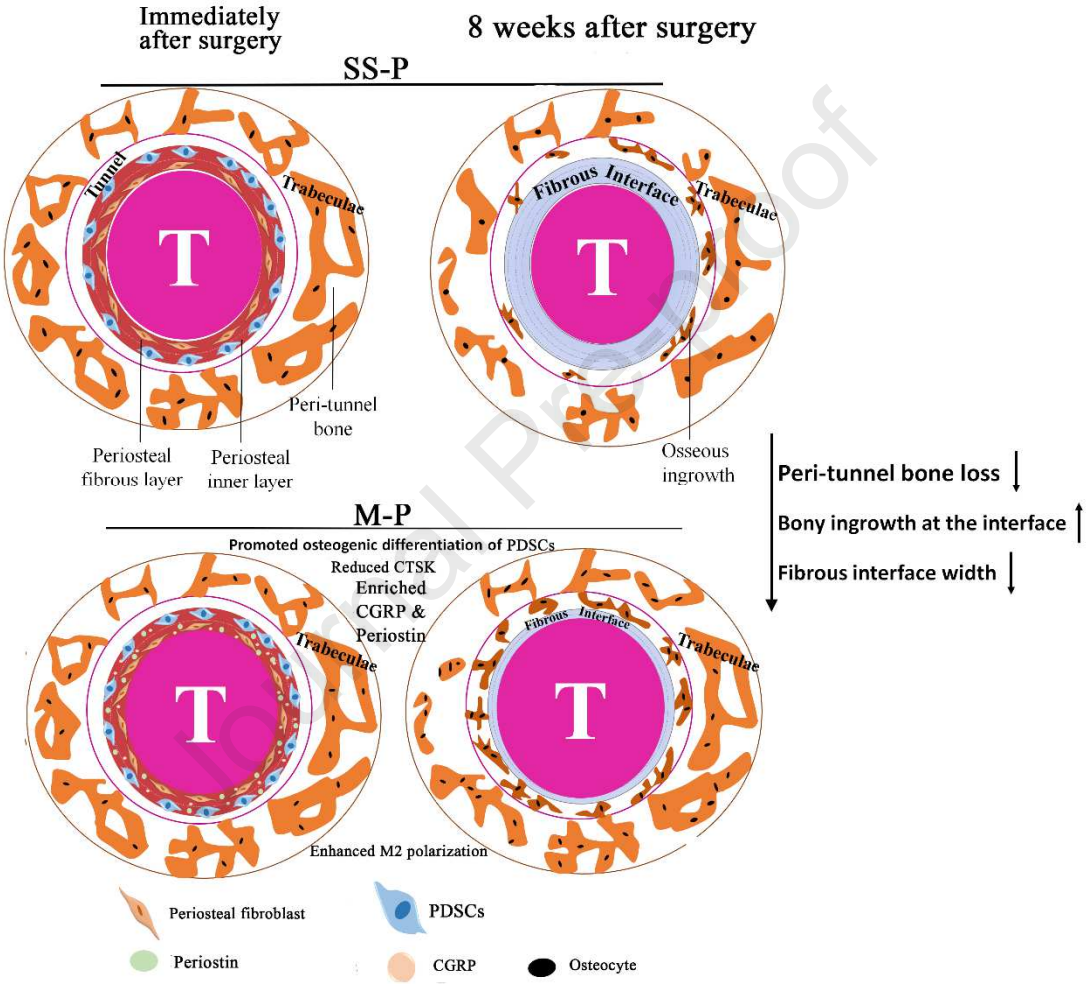


**Figure 9**. Schematic diagram of mechanisms behind the promotive effects of the Mg-pretreated periosteum in the tendon-bone healing. The expression levels of CGRP and periostin as well as macrophage towards M2 polarization were upregulated under the stimuli of Mg ions, ultimately leading to less fibrous interface and peri-tunnel bone loss, and more fibrocartilage formation as an important template for the replacement by new bone in the M-P group when compared to the SS-P group.

Since the strength of the tendon-bone interface has been shown to correlate with the amount of the osseous ingrowth [7], current attempts have been made to enhance the osteointegration of the tendon graft into the bone tunnel [8, 9, 16]. Periosteum is composed of two layers, that is outer fibrous layer (containing fibroblasts) and inner cambium layer (extremely rich in mesenchymal progenitor cells). Fibrous layer

contributes to formation of collagen fibers while cambium layer forms fibrocartilage and bone[23]. As a pool of multipotent mesenchymal stem cells [31], periosteum regulates the outer shape of the cortical bone and also remarkably affects the fracture repair via endochondral and intramembranous ossification [32], suggesting its potential in the tendon-bone healing. As early as in 1930, Burman and Umansky found that bone formation was observed at the periosteum-tendon interface at 2 weeks after surgery when the periosteum was wrapped around the extensor longus digitorum tendon, indicating the contributions of the periosteum to initiation of bone regeneration [33]. Later on, Chen et al. tried to suture the periosteum onto the surface of the tendon portion for ACL reconstruction in rabbits and found better healed strength [16], which was partially ascribed to the beneficial effects of PDSCs in periosteum on new bone formation at the interface [34]. Encouraged by the findings in the animal studies, Chen et al. continued to carry out clinical studies by using periosteum-enveloping tendon graft in patients and got improved clinical outcomes via observation of reduced bone tunnels [17, 18]. In addition, periosteum is rich in sensory nerves, which regulate bone formation via release of neuropeptides such as CGRP [35]. We previously found that Mg could significantly stimulate CGRP expression during the early stage of fracture healing [19]. In that study, we found that the Mg ions released from the Mg rod shortly after implantation and speculated that these Mg ions transported into the neurons through ion channels/transporters such as Mg transporter 1 (MagT1) [19]. The influx of Mg ions rapidly stimulated the release of CGRP from the nerve endings through elevating ATP-related pathways [19], thus serving as the molecular basis for explaining the short-term reaction of Mg on CGRP. Therefore, the CGRP enriched periosteum through Mg pretreatment was used to wrap the tendon graft, aiming to improve the bony ingrowth towards the tendon-bone interface in this study. As expected, our current proof-of-concept study showed that the periosteum pretreated by Mg implants for 2 weeks possessed the peak expression of CGRP , so we prepared the CGRP enriched periosteum at week 2 after surgery for our *in vivo* validation. In addition, as the predominant extracellular matrix in the periosteum, we found that periostin also directly promoted the osteogenic differentiation of PDSCs, consistent with findings from another study using a different cell model [26]. As a direct molecular target for degradation by CTSK [36], periostin was well protected by Mg ions through negative modulation of CTSK.

The SS and Mg treatment outcomes were then systematically investigated in ACL reconstruction animal models. Generally, the peri-tunnel bone loss after ACL reconstruction is commonly observed in both preclinical and clinical studies, which is considered to adversely affect the tendon graft healing due to the impaired stability in the bone tunnel healing surface during tendon-bone integration [37]. Compared to the SS-pretreated periosteum, the Mg-pretreated periosteum *in vivo* or *in situ* significantly attenuated the peri-tunnel bone loss in the M-P group after surgery, indicating a more stable bone tunnel surface to facilitate the tendon graft healing and integration. More importantly, massive fibrocartilage was formed at the tendon-bone interface in the M-P group while only fibrous interface was observed in the SS-P group at week 4 after surgery. Further, we tried to investigate how the treated periosteum exert its

biological effects in the tendon-bone healing process, so we isolated the Mg- or SS-pretreated periosteum and then prepared the periosteum-tendon graft complex *in vivo* to observe their interactions. Interestingly, we found fibrocartilage-like tissue only formed at the complex interface in the M-P group. This may be partially ascribed to the enhanced osteogenic differentiation of PDSCs in the Mg-pretreated periosteum, which provided the cell source involved in the interaction with the local tendon derived fibroblasts [38]. However, we can still not exclude the potential interaction between the periosteum and the surrounding bone in ACL reconstruction model. We may consider use transgenic animal models such as *Prx1CreER-EGFP* mice to conduct lineage tracing to get more information on the fate of stem cells during the tendon-bone healing in the future. The fibrocartilage at the tendon-bone interzone structure served as the template for the replacement by new bone gradually in the presence of bone marrow derived stem cells [39, 40] and ultimately contributed to increased osseous ingrowth into the tendon-bone interface in the M-P group as compared to the SS-P group at week 8 after operation. Of note, there was only marginal significant difference in the fibrous interface width and the peri-tunnel bone loss ($P = 0.051$) at 8 weeks after the surgery, implying the possibility that CGRP and periostin in the harvested periosteum might be rapidly exhausted instead of released in a controlled manner over time, warranting further optimization for future application.

Dagher et al. reported that the increased polarization of M2 macrophage at the tendon-bone interface contributed to the diminished width of the fibrous tissue [41]. After Mg treatment, the polarization of macrophages toward M2 was remarkably favored, leading to a reduction of excessive inflammation during the graft healing. Consequently, compared to the SS-pretreated periosteum, the Mg-pretreated periosteum significantly reduced the fibrous interface width while promoted the bony ingrowth and peri-tunnel bone formation at the tendon-bone interface in rabbits with ACL reconstruction, which ultimately leading to a significant increase in the bonding strength between the tendon graft and the bone tunnel according to the tensile testing results.

Last but not the least, there are also a few limitations in our proof-of-concept study. Firstly, an additional surgery is required for harvesting the Mg-pretreated periosteum prior to ACL reconstruction, causing injury at the donor site. However, it is an indispensable step to conduct this test as proof-of-concept. Our data promisingly confirmed the beneficial effects of CGRP and periostin delivered in Mg-treated periosteum, which has opened a new avenue for future translational research and application by developing relevant delivery systems, e.g. using injectable hydrogel for encapsulating the CGRP, periostin and cells for ACL reconstruction [27]. Secondly, as there is lack of commercial primary antibody to target periostin in rabbits, we alternatively used rat model to measure the effect of Mg on periostin expression. Our previous study showed that Mg ions significantly increased the concentration of CGRP in the periosteal layer in rats after surgery [19], similar to the current result from rabbit model, suggesting its biological responses and Mg ion release pattern between rats and rabbits would be comparable. Considering that μXRF requires flat polished surface of specimens for testing, it would raise huge difficulty in preparation

of larger specimens, so we only selected the rat specimen to measure the proportion of Mg/Ca in this study.

## 5. Conclusions

In the current study, Mg-pretreated periosteum (M-P) significantly enhanced the osteointegration of the tendon graft into the bone tunnels in rabbits as compared to the SS-P group. The enhanced osteogenic differentiation of PDSCs may be attributed to the upregulated expression of CGRP and periostin after Mg treatment. Our findings suggest that local delivery of CGRP, periostin, and stem cells may be a promising strategy for improving the tendon-bone healing in patients undergoing ACL reconstruction.

## Author Contributions

L.Q., J.W., and J.X. designed and conducted all the experiments. X.W. and L.S. assisted to conduct the *in vitro* studies. B.S., R.Z., H.Y., N.Z., L.Z., and P.Y. performed surgeries. G.W. assisted to do μXRF in bone. T.O. conducted histological analysis. J.W. and J.X. wrote the manuscript. All authors discussed the data and commented on the manuscript.

## Declaration of competing interest

The authors declare no competing financial interests.

## Acknowledgements

This work was supported by the National Natural Science Foundation of China (Ref No. 81702165 and 81802152), Guangdong Natural Science Fund (Ref. No. 2019A1515011404), Key-Area Research and Development Program of Guangdong Province (Ref. No. 2020B090924004), and Theme-based Research Scheme (Ref No. T13-402/17-N) from the Research Grants Council of Hong Kong Special Administrative Region, China.

### References

[1] A. von Porat, E.M. Roos, H. Roos, High prevalence of osteoarthritis 14 years after an anterior cruciate ligament tear in male soccer players: a study of radiographic and patient relevant outcomes, Ann Rheum Dis 63(3) (2004) 269-273.

[2] W.P. Li, Y. Song, B. Song, R. Yang, T. Xing, Z. Chen, Z.Z. Zhang, Y. Ouyang, Comparison of anterior cruciate ligament reconstruction methods between reverse "Y" plasty reconstruction and traditional single-bundle technique-A cadaveric study, Journal of Orthopaedic Translation 14 (2018) 1-7.

[3] P.N. Chalmers, N.A. Mall, M. Moric, S.L. Sherman, G.P. Paletta, B.J. Cole, B.R. Bach, Does ACL Reconstruction Alter Natural History? A Systematic Literature Review of Long-Term Outcomes, Journal of Bone and Joint Surgery-American Volume 96a(4) (2014) 292-300.

[4] S.N. Crawford, B.R. Waterman, J.H. Lubowitz, Long-Term Failure of Anterior Cruciate Ligament Reconstruction, Arthroscopy-the Journal of Arthroscopic and Related Surgery 29(9) (2013) 1566-1571.

[5] C.L. Ardern, N.F. Taylor, J.A. Feller, K.E. Webster, Fifty-five per cent return to competitive sport following anterior cruciate ligament reconstruction surgery: an updated systematic review and meta-analysis including aspects of physical functioning and contextual factors, Br J Sports Med 48(21) (2014) 1543-52.

[6] J. Menetrey, V.B. Duthon, T. Laumonier, D. Fritschy, "Biological failure" of the anterior cruciate ligament graft, Knee Surg Sport Tr A 16(3) (2008) 224-231.

[7] S.A. Rodeo, S.P. Arnoczky, P.A. Torzilli, C. Hidaka, R.F. Warren, Tendon-healing in a bone tunnel. A biomechanical and histological study in the dog, J Bone Joint Surg Am 75(12) (1993) 1795-803.

[8] R. Mihelic, M. Pecina, M. Jelic, S. Zoricic, V. Kuseo, P. Simic, D. Bobinac, B. Lah, D. Legovic, S. Vukicevic, Bone morphogenetic protein-7 (Osteogenic protein-1) promotes tendon graft integration in anterior cruciate ligament reconstruction in sheep, Am J Sport Med 32(7) (2004) 1619-1625.

[9] K. Anderson, A.M. Seneviratne, K. Izawa, B.L. Atkinson, H.G. Potter, S.A. Rodeo, Augmentation of tendon healing in an intraarticular bone tunnel with use of a bone growth factor, Am J Sport Med 29(6) (2001) 689-698.

[10] A. Weiler, C. Forster, P. Hunt, R. Falk, T. Jung, F.N. Unterhauser, V. Bergmann, G. Schmidmaier, N.P. Haas, The influence of locally applied platelet-derived growth factor-BB on free tendon graft remodeling after anterior cruciate ligament reconstruction, Am J Sports Med 32(4) (2004) 881-91.

[11] T. Yoshikawa, H. Tohyama, T. Katsura, E. Kondo, Y. Kotani, H. Matsumoto, Y. Toyama, K. Yasuda, Effects of local administration of vascular endothelial growth factor on mechanical characteristics of the semtendinosus tendon graft after anterior cruciate ligament reconstruction in sheep, Am J Sport Med 34(12) (2006) 1918-1925.

[12] K. Sasaki, R. Kuroda, K. Ishida, S. Kubo, T. Matsumoto, Y. Mifune, K. Kinoshita, K. Tei, T. Akisue, Y. Tabata, M. Kurosaka, Enhancement of tendon-bone osteointegration of anterior cruciate ligament graft using granulocyte colony-stimulating factor, Am J Sport Med 36(8) (2008) 1519-1527.

[13] M. Cervellin, L. de Girolamo, C. Bait, M. Denti, P. Volpi, Autologous platelet-rich plasma gel to reduce donor-site morbidity after patellar tendon graft harvesting for anterior cruciate ligament reconstruction: a randomized, controlled clinical study, Knee Surg Sports Traumatol Arthrosc 20(1) (2012) 114-20.

[14] A. Vadala, R. Iorio, A. De Carli, M. Ferretti, D. Paravani, L. Caperna, C. Iorio, A. Gatti, A. Ferretti, Platelet-rich plasma: does it help reduce tunnel widening after ACL reconstruction?, Knee Surg Sport Tr A 21(4) (2013) 824-829.

[15] C. Colnot, Skeletal Cell Fate Decisions Within Periosteum and Bone Marrow During Bone Regeneration (vol 24, pg 274, 2009), Journal of Bone and Mineral Research 24(4) (2009) 758-758.

[16] C.H. Chen, W.J. Chen, C.H. Shih, C.Y. Yang, S.J. Liu, P.Y. Lin, Enveloping the tendon graft with periosteum to enhance tendon-bone healing in a bone tunnel: A biomechanical and histologic study in rabbits, Arthroscopy 19(3) (2003) 290-6.

[17] C.H. Chen, C.H. Chang, C.I. Su, K.C. Wang, H.T. Liu, C.M. Yu, C.B. Wong, I.C. Wang, Arthroscopic single-bundle anterior cruciate ligament reconstruction with periosteum-enveloping hamstring tendon graft: clinical outcome at 2 to 7 years, Arthroscopy 26(7) (2010) 907-17.

[18] C.H. Chen, W.J. Chen, C.H. Shih, S.W. Chou, Arthroscopic anterior cruciate ligament reconstruction with periosteum-enveloping hamstring tendon graft, Knee Surg Sports Traumatol Arthrosc 12(5) (2004) 398-405.

[19] Y. Zhang, J. Xu, Y.C. Ruan, M.K. Yu, M. O'Laughlin, H. Wise, D. Chen, L. Tian, D. Shi, J. Wang, S. Chen, J.Q. Feng, D.H. Chow, X. Xie, L. Zheng, L. Huang, S. Huang, K. Leung, N. Lu, L. Zhao, H. Li, D. Zhao, X.

Guo, K. Chan, F. Witte, H.C. Chan, Y. Zheng, L. Qin, Implant-derived magnesium induces local neuronal production of CGRP to improve bone-fracture healing in rats, Nat Med 22(10) (2016) 1160-1169.
[20] J.L. Wang, J.K. Xu, C. Hopkins, D.H.K. Chow, L. Qin, Biodegradable Magnesium-Based Implants in Orthopedics-A General Review and Perspectives, Adv Sci (2020).
[21] J.L. Wang, J.K. Xu, B. Song, D.H. Chow, P.S.H. Yung, L. Qin, Magnesium (Mg) based interference screws developed for promoting tendon graft incorporation in bone tunnel in rabbits, Acta Biomater 63 (2017) 393-410.
[22] J.B. Qin, F.K. Yuan, Z.Y. Peng, K.C. Ye, X.R. Yang, L.J. Huang, M. Yang, X.W. Lu, Periostin enhances adipose-derived stem cell adhesion, migration, and therapeutic efficiency in Apo E deficient mice with hind limb ischemia, Stem Cell Research & Therapy 6 (2015) 108-119.
[23] O. Duchamp de Lageneste, A. Julien, R. Abou-Khalil, G. Frangi, C. Carvalho, N. Cagnard, C. Cordier, S.J. Conway, C. Colnot, Periosteum contains skeletal stem cells with high bone regenerative potential controlled by Periostin, Nat Commun 9(1) (2018) 773.
[24] J. Wang, J. Xu, W. Fu, W. Cheng, K. Chan, P.S. Yung, L. Qin, Biodegradable Magnesium Screws Accelerate Fibrous Tissue Mineralization at the Tendon-Bone Insertion in Anterior Cruciate Ligament Reconstruction Model of Rabbit, Sci Rep 7 (2017) 40369.
[25] J.L. Wang, Y.H. Wu, H.F. Li, Y. Liu, X.L. Bai, W.H. Chau, Y.F. Zheng, L. Qin, Magnesium alloy based interference screw developed for ACL reconstruction attenuates peri-tunnel bone loss in rabbits, Biomaterials 157 (2018) 86-97.
[26] Y. Tang, L. Liu, P. Wang, D. Chen, Z. Wu, C. Tang, Periostin promotes migration and osteogenic differentiation of human periodontal ligament mesenchymal stem cells via the Jun amino-terminal kinases (JNK) pathway under inflammatory conditions, Cell proliferation 50(6) (2017).
[27] Q. Feng, J. Xu, K. Zhang, H. Yao, N. Zheng, L. Zheng, J. Wang, K. Wei, X. Xiao, L. Qin, L. Bian, Dynamic and Cell-Infiltratable Hydrogels as Injectable Carrier of Therapeutic Cells and Drugs for Treating Challenging Bone Defects, ACS central science 5(3) (2019) 440-450.
[28] J.K. Xu, H.J. Chen, X.D. Li, Z.L. Huang, H. Xu, H.L. Yang, J. Hu, Optimal intensity shock wave promotes the adhesion and migration of rat osteoblasts via integrin beta1-mediated expression of phosphorylated focal adhesion kinase, The Journal of biological chemistry 287(31) (2012) 26200-12.
[29] J. Wang, F. Witte, T. Xi, Y. Zheng, K. Yang, Y. Yang, D. Zhao, J. Meng, Y. Li, W. Li, K. Chan, L. Qin, Recommendation for modifying current cytotoxicity testing standards for biodegradable magnesium-based materials, Acta Biomater 21 (2015) 237-49.
[30] P.L. Hays, S. Kawamura, X.H. Deng, E. Dagher, K. Mithoefer, L. Ying, S.A. Rodeo, The role of macrophages in early healing of a tendon graft in a bone tunnel, J Bone Joint Surg Am 90(3) (2008) 565-79.
[31] C. De Bari, F. Dell'Accio, J. Vanlauwe, J. Eyckmans, I.M. Khan, C.W. Archer, E.A. Jones, D. McGonagle, T.A. Mitsiadis, C. Pitzalis, F.P. Luyten, Mesenchymal multipotency of adult human periosteal cells demonstrated by single-cell lineage analysis, Arthritis Rheum 54(4) (2006) 1209-21.
[32] M.R. Allen, J.M. Hock, D.B. Burr, Periosteum: biology, regulation, and response to osteoporosis therapies, Bone 35(5) (2004) 1003-12.
[33] M.S. Burman, M. Umansky, An experimental study of free periosteal transplants, wrapped around tendon: With a review of the literature. , J Bone Joint Surg Am 12 (1930) 579-594.
[34] C.H. Chen, H.W. Liu, C.L. Tsai, C.M. Yu, I.H. Lin, G.H. Hsiue, Photoencapsulation of bone morphogenetic protein-2 and periosteal progenitor cells improve tendon graft healing in a bone tunnel, Am J Sports Med 36(3) (2008) 461-73.

[35] K. Irie, F. Hara-Irie, H. Ozawa, T. Yajima, Calcitonin gene-related peptide (CGRP)-containing nerve fibers in bone tissue and their involvement in bone remodeling, Microsc Res Techniq 58(2) (2002) 85-90.

[36] N. Bonnet, J. Brun, J.C. Rousseau, L.T. Duong, S.L. Ferrari, Cathepsin K Controls Cortical Bone Formation by Degrading Periostin, Journal of bone and mineral research : the official journal of the American Society for Bone and Mineral Research 32(7) (2017) 1432-1441.

[37] P.P.Y. Lui, Y.W. Lee, T.Y. Mok, Y.C. Cheuk, K.M. Chan, Alendronate Reduced Peri-Tunnel Bone Loss and Enhanced Tendon Graft to Bone Tunnel Healing in Anterior Cruciate Ligament Reconstruction, Eur Cells Mater 25 (2013) 78-96.

[38] I.E. Wang, H.H. Lu, Role of cell-cell interactions on the regeneration of soft tissue-to-bone interface, Conf Proc IEEE Eng Med Biol Soc 1 (2006) 783-6.

[39] D.L. Bunker, V. Ilie, V. Ilie, S. Nicklin, Tendon to bone healing and its implications for surgery, Muscles Ligaments Tendons J 4(3) (2014) 343-50.

[40] Y.G. Li, J.N. Wei, J. Lu, X.T. Wu, G.J. Teng, Labeling and tracing of bone marrow mesenchymal stem cells for tendon-to-bone tunnel healing, Knee Surg Sports Traumatol Arthrosc 19(12) (2011) 2153-8.

[41] E. Dagher, P.L. Hays, S. Kawamura, J. Godin, X.H. Deng, S.A. Rodeo, Immobilization Modulates Macrophage Accumulation in Tendon-Bone Healing, Clinical Orthopaedics and Related Research 467(1) (2009) 281-287.

**Declaration of interests**

☒ The authors declare that they have no known competing financial interests or personal relationships that could have appeared to influence the work reported in this paper.

☐The authors declare the following financial interests/personal relationships which may be considered as potential competing interests: